Available online at www.sciencedirect.com

ScienceDirect

Energy Procedia 158 (2019) 4502–4509

Energy Procedia

www.elsevier.com/locate/procedia

10th International Conference on Applied Energy (ICAE2018), 22-25 August 2018, Hong Kong, China

A Numerical Investigation into the Heat Transfer and Melting Process of Lauric Acid in a Rectangular Enclosure with Three Values of Wall Heat Flux

Mohamed Fadl* and Philip Eames

Centre for Renewable Energy Systems Technologies (CREST),
Wolfson School of Mechanical, Electrical and Manufacturing Engineering,
Loughborough University, Leicestershire LE11 3TU, UK

Abstract

A numerical study of melting of Lauric acid in a vertical rectangular cross-section enclosure was performed with FLUENT 18.2. The enclosure was subject to a constant heat flux on one side of 500, 750 and 1000 W/m^2. For model validation purposes simulations were initially performed of experimental systems in the literature with predicted values compared to experimental measurements. Predictions indicate that during the initial stage of melting, conduction is the dominant mode of heat transfer, subsequently replaced by convection when there is sufficient liquid PCM. The simulations show that as the magnitude of heat flux is increased, average wall temperature increases and melting time reduces. The predicted results indicated that melting time decreases by 28.5 % as the wall flux increases by 50 % from 500 to 750 W/m^2. The time required for melting reduces by about 50% when the wall heat flux is increased from 500 to 1000 W/m^2.

Keywords: Melting, PCM, Wall heat flux, Rectangular enclosure.

1. Introduction

Energy storage plays an important role in improving performance, applicability and reliability of variable renewable energy sources helping to reduce the mismatch between supply and demand [1]. Storage is especially important in solar energy applications because of the seasonal, diurnal, and intermittent nature of the solar resource.

* *Corresponding author. Tel: +44 01509 635609*
E-mail address: m.s.fadl@lboro.ac.uk

10.1016/j.egypro.2019.01.761

For solar systems, thermal energy storage systems (TESS) are suitable for use with solar thermal collectors. Thermal energy storage can be in the form of sensible heat in a liquid or solid medium achieved by increasing its temperature without change of phase [2] or latent heat utilising the heat required to change phase, generally from solid to liquid in Phase Change Materials, (PCMs).

Nomenclature	
A_{mush}	Mushy zone constant (kg/s m^3)
Cp	Specific heat at constant pressure (J/kg ^oC)
g	Gravitational acceleration (m/s^2)
H	Specific enthalpy (J/Kg)
K	Thermal conductivity (W/m ^oC)
PCM	Phase change material
T	Temperature (^oC)
t	Time (s)
L	Latent heat (J/Kg)
V	Fluid velocity (m/s)
Greek symbols	
β	Volumetric liquid fraction of the PCM
γ	Thermal expansion ($^oC^{-1}$)
ε	Constant
μ	Dynamics viscosity (Kg/m s)
ρ	Density (Kg/m^3)

Thermal energy storage using PCMs is an efficient way of storing heat if the operational temperature range that can be used is restricted, providing higher heat storage capacity in a given volume. Lower peak storage temperatures reduce rates of heat loss. Utilising phase change also theoretically allows nearly constant temperature discharge to be achieved.

The growth of interest in design and optimization of latent heat thermal energy storage (LHTES) systems supports the need for extensive analysis and better understanding of the movement of the solid-liquid interface and associated heat transfer during melting and solidification (conduction, convection or a combination of the two), which take place during phase transformations within the PCM and the heat transfer at the boundary, commonly either constant wall temperature (CWT) or constant wall flux (CWF) [3].

Different geometries have been suggested for PCM thermal storage systems including rectangular, spherical and cylindrical containers. H. Sattari et al [4] simulated numerically melting of PCMs in a spherical containers, the simulations indicated that the container's surface temperature effects melting rate more than other parameters (container diameter, initial temperature and Stefan number) and at the start of the melting process, heat conduction is the dominant mode of heat transfer. S. Seddegh et al [5] performed experimental studies into the effect of geometric design on vertical shell and tube LHTES systems (cylindrical and conically shaped) and showed that the conically shaped system can store thermal energy much faster than a cylindrical system due to the conical design increasing natural convection in the large volume of PCM at the top of the container. There was no significant difference during the discharging process. G. Han et al [6] numerically investigated the effect of natural convection (NC) on the melting process in different shell-and-tube latent heat thermal energy storage systems (with fixed volume/mass of PCM). Results indicate that NC can cause a non-uniform solid/liquid interface, which accelerates the rate of PCM melting. The predicted rate of heat transfer to the PCM and the rate of melting are higher in the horizontal cylinder model than those in the horizontal cylinder model because of the combined effects of heat conduction and NC.

Heat storage units with rectangular cross section are important in areas including solar energy system, nuclear reactors, geothermal energy, etc., because of their simplicity[7]. A number of experimental studies have been conducted to understand the phase change process, in particular the solid/liquid position and temperature field during the melting and solidification. H. Shokouhmand and B. Kamkari [8] conducted an experimental analysis to visualize the temperature field and melt front development during the melting process of lauric acid ($C_{12}H_{24}O_2$) in a rectangular thermal storage unit with vertical walls of uniform temperature. They observed that, during the initial stage of melting, heat conduction was the dominant mode of heat transfer, followed by a transition from conduction to convection, and finally to convection dominated heat transfer. The same investigators [9] experimentally investigated the influence of enclosure inclination angle (0°,45° and 90°) and hot wall temperature (55, 60 and 70°C)

on natural convection heat transfer and solid/liquid interface location during phase change. They found that enclosure inclination angle has a significant effect on the formation of natural convection currents, heat transfer rate and the melting time of the PCM. P.H. Biwole et al [10] performed a numerical analysis of the melting process to determine the effects of the number, dimension and position of fins in a rectangular enclosure with a constant wall heat flux of 1000W/m^2 on PCM melting. They found that increasing the number of fins diminishes both the maximum temperature of the front plate and the time to achieve it during phase change and accelerates the rate of both sensible and latent heat storage in the PCM due to increased contact surface area between the fins and the PCM.

The present paper reports the simulation of melting of Lauric acid in an enclosure of rectangular cross-section with three different values of wall heat flux applied to the right vertical wall on the natural convective flow structures and heat transfer and melting rates.

2. Modelled System

The two-dimensional system geometry modelled is presented in Fig.1. The design and dimensions of the PCM enclosure containing Lauric acid used in the simulations are similar to those used in the experimental study undertaken by H. Shokouhmand and B. Kamkari [8]. In the experimental study, PCM melting was quantified by visually tracking the shape of the liquid-solid interface and how it changed with time. The container depicted in Figure.1 had a rectangular cross-section with inside dimensions of 0.05 m width, 0.12 m height and 0.12 depth, the enclosure is heated from the right wall with constant normal heat fluxes of q_w=500, 750 and 1000 W/m^2 for the duration of the simulation. The other three walls of the enclosure were made from 0.025 m thick plexiglass with a thermal conductivity k of 0.043 W/m K. The system was initially all at a temperature T_0=293.15 K. Since renewable energy heat sources, for example, many solar thermal systems and shallow geothermal operate at temperatures below 60°C a PCM with a low melting point may be appropriate for a range of applications. A Lauric acid of 99 % purity was the PCM used in this study because of its well- defined thermophysical properties[8] as shown in Table 1.

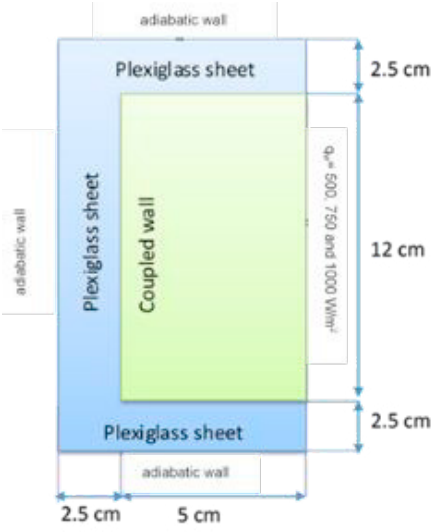

Fig.1. A schematic diagram of the simulation geometry with details of the imposed boundary conditions

Table 1. Thermophyscial properties of Lauric acid

	Solid	Liquid
T (K)	316.65	321.35
ρ (kg/m^3)	940	885
C_p (J/Kg K)	2180	2390
k (W/m K)	0.16	0.14
μ_l (kg / m s)		0.008
γ (K^{-1})	0.0008	
L (J/Kg)	187210	

3. The numerical model

The numerical approach adopted enables prediction of natural convection that occurs in the liquid PCM during the melt process. In the approach used to simulate melting, the flow was considered to be unsteady, laminar, incompressible and two-dimensional. It was assumed that both solid and liquid phases are homogeneous and isotropic.

$$\frac{\partial \rho}{\partial t} + \nabla.(\rho V) = 0 \qquad (1)$$

$$\frac{\partial(\rho V)}{\partial t} + \nabla.(\rho V) = -\nabla p + \mu\nabla^2 V + \rho g + S \quad (2)$$

$$\frac{\partial(\rho H)}{\partial t} + \nabla.(\rho V H) = k\nabla^2 T \quad (3)$$

The enthalpy–porosity approach [11] was adopted for simulation of the PCM. The governing conservation equations used for the PCM system are:

$$H = h + \Delta H \quad (4)$$

Where:

$$h = h_{ref} + \int_{T_{ref}}^{T} C_p dT \quad (5)$$

Where h_{ref} is the reference enthalpy at the reference temperature T_{ref}, C_p is the specific heat capacity. The latent heat can vary between zero (for a solid) and L (for a liquid):

$$\Delta H = \beta L \quad (6)$$

Where the liquid fraction (β) is given by the following equations:

$$\beta = \begin{cases} 0 & if\ T < Ts \\ \frac{T - T_S}{T_l - T_s} & if\ T_s < T < T_l \\ 1 & if\ T > Tl \end{cases} \quad (7)$$

The source term $\vec{S}$ in the momentum equation, Eq. (2), is given by:

$$\vec{S} = -A(\beta)\vec{V} \quad (8)$$

where A(β) is the ‘‘porosity function” defined by Brent et al [12]. The source term was used in the momentum equation to describe the flow in the porous medium, It has to be set to zero in the liquid phase to allow for free motion, but it has to be sufficiently large in the solid phase to force the velocity values to near zero values [13]. While different functions fulfil this requirement, the most used is the modified form of the Carman-Kozeny equation, which is derived from the Darcy law for fluid flow in porous media:

$$A(\beta) = \frac{A_{mush}\,(1-\beta)^2}{\beta^3 + \varepsilon} \quad (10)$$

Where ε is a small computational constant used to prevent zero in the denominator (in this work ε = 0.001), and A_{mush} is the mushy zone constant which determines how fast the fluid velocity approaches zero as it solidifies.

4. Computational procedure and validation

The simulations were performed using the ANSYS FLUENT 18.2 software, run as a two-dimensional double precision (2ddp) code. The pressure based coupled algorithm was used to solve the momentum and continuity equations. The gravity vector was set to -9.8 m/s^2 in the y-direction for prediction of natural convection in the PCM when liquid. A second-order upwind scheme for the advection term, central differencing for the diffusion term and a second order implicit discretization scheme for the transient term were used. The PRESTO pressure interpolation scheme for the transient calculations was implemented. The under-relaxation factors for density, momentum, pressure correction, thermal energy and melt fraction used were 1, 0.7, 0.3, 1 and 0.9, respectively. The mesh was generated using the mesh generator ICEM CFD. The effects of time step size, A_{mush} and grid size on the solution were carefully examined in preliminary calculations. A fine mesh composed quadrilateral mesh geometry was selected using13500 elements and a time step of 0.2 sec were deemed to give satisfactory mesh independent results.

Simulations were conducted on the Loughborough University High-Performance Computing (HPC) Research cluster which consists of 7 compute nodes, each having two six-core Intel Westmere Xeon X5650 CPUs and 24 GB of memory. A typical simulation to achieve complete melting required from 50 hours to 100 hours of computing time.

The numerical model described above has been compared to the results from the experiments of H. Shokouhmand [8] with the exception that the right wall is maintained at a temperature T_w=343.15 K. the validation is based on the comparison of the simulated and actual melt fraction values as shown in Figures 2 and 3.

The simulations undertaken show that higher A_{mush} (>10^6) values result in low melting rates and for low values of A_{mush} (<10^5), the melting rate increases significantly. For an A_{mush} value of 5x10^5, the melt interface curvature more accurately resembles that of the experimental results, this supports the selection of an A_{mush} value of 5x10^5 to be optimal out of the five values tested.

5. Results and discussion

Figures 4 and 5 present the predicted melt fraction and surface wall temperature with time for the 3 values of wall heat flux (500, 750 and 1000 W/m^2) imposed at the right wall.

It is clear from Figures 4 and 5 that as the wall heat flux increases, the total melting time reduces. This is expected behavior due to the larger rate of heat transfer to the enclosure. The increase in heat flux has also led to an increase in the average wall surface temperature. As the wall flux increases from 500 to 750 W/m^2 (by 50 %), melting time decreases by 28.5 %. The time required for melting reduces by about 50% when wall heat flux is increased from 500 to 1000 W/m^2.

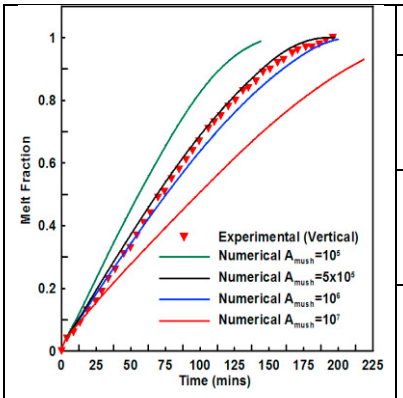

Figure 2 Melt fraction with time for selected values of the mushy zone parameter, A_{mush} during the charging process.

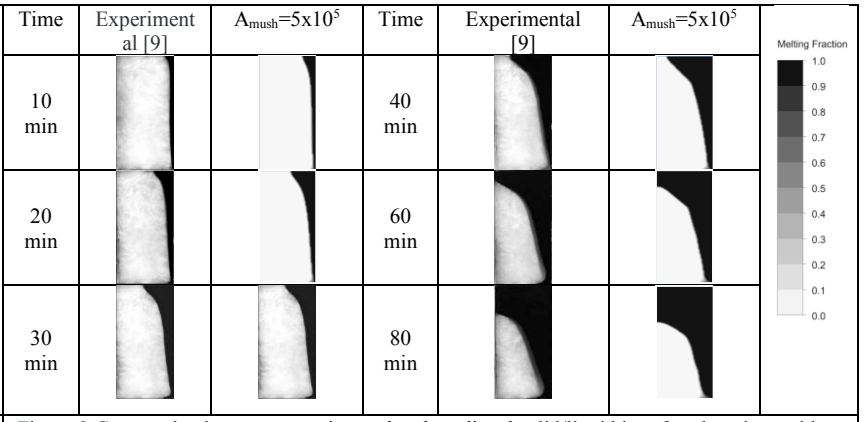

Figure 3 Comparsion between experimental and predicted solid/liquid interface locations with time for $A_{mush,}$ =5x10^5

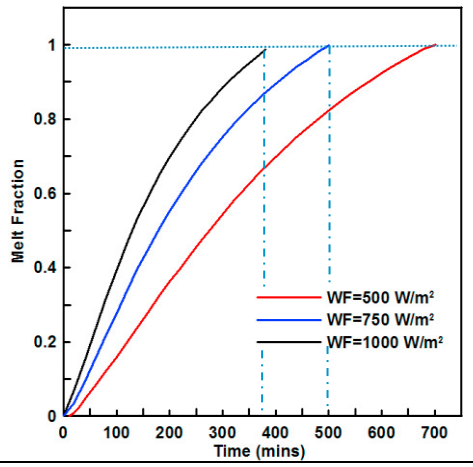

Figure 4. Melt fraction with time for three values of wall heat flux (500, 750 and 1000 W/m^2)

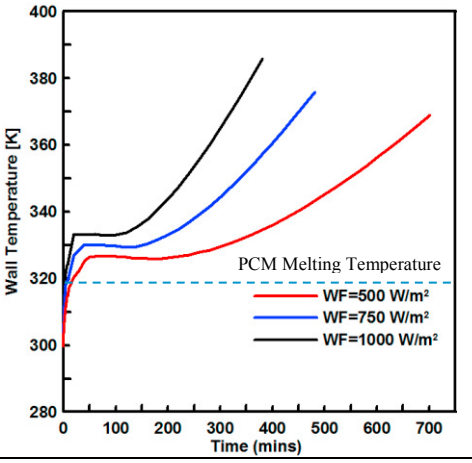

Figure 5. Predicted wall surface temperatures for three values of wall heat flux (500, 750 and 1000 W/m^2)

The simulation results show that in the early stages of melting (< 30 mins), conduction is the main heat transfer mode inside the PCM. From Figure 5 during this time the wall temperature increase is nearly linear, after 30 mins, melting occurs adjacent to the wall and natural convection starts to drive the molten PCM upwards due to the density

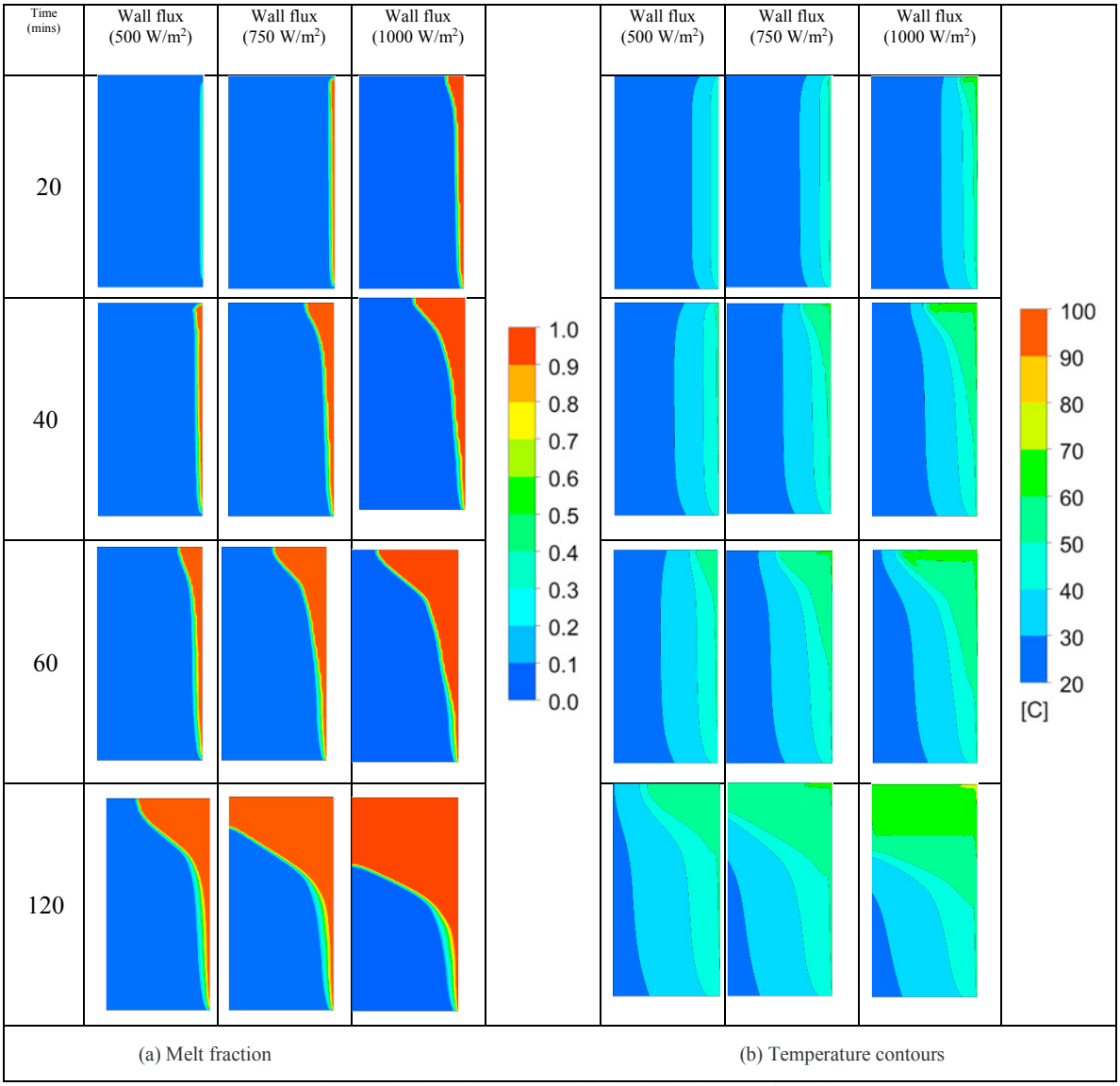

Figure 6. Simulated temperature field and melt front at selected times

gradient between the hotter and colder liquid PCM. As melting progresses, natural convection driven fluid flow increases, transferring more heat, melting the solid PCM and increasing the liquid fraction. As heat is transferred more rapidly to the PCM, the rate of increase of average wall temperature reduces. The strength of convective flow increases with increasing input wall flux.

Figure 6 (a and b) presents the predicted temperature contours and the locations of the solid-liquid interface for the three different wall heat fluxes. In the initial stage of melting, a thin layer of liquid PCM forms adjacent to the heated surface, at this stage conduction is the dominant heat transfer mechanism. Conduction dominates as long as the viscous forces exceed the buoyancy forces, inhibiting fluid motion, the melt front remains almost uniformly wide and parallel to the hot surface. As time progresses, the thickness of the liquid PCM increases, the buoyancy forces

exceed the viscous forces and convection establishes a circulation in the liquid region. Heat transfer to the liquid PCM adjacent to the heated surface increases its temperature, reducing its density and it rises. At the top container surface, it is deflected and flows to the solid PCM subsequently descending along the solid-liquid interface, melting the solid PCM at the interface and forming the interface shape.

Figure 6-b presents the predicted temperature distribution in the vertical plane through the enclosure, during the initial stage of melting, the temperature contours are almost parallel to the vertical heated surface, indicating that heat transfer is mainly by conduction. As time elapses, the amount and temperature of the liquid PCM adjacent to the hot surface increases while its density decreases causing the liquid PCM adjacent to the hot surface to rise until it reaches the top of the melt layer. It is then deflected and descends along the solid-liquid interface, heat transfer causing its temperature to decrease. The change in direction of the liquid flow at the top surface of the enclosure leads to the inclination of the temperature contours.

6. Conclusions

This paper presents the results of a two-dimensional transient numerical simulation of the thermal behavior of a PCM, Lauric acid melting in a vertical rectangular enclosure with an imposed heat flux of (500, 750 and 1000 W/m^2) on the heated wall surface. The model validation was undertaken with predictions comparing well with the experimental data from the literature. The following concluding remarks can be drawn from the obtained results.

- A_{mush} is an important parameter if seeking to accurately model phase change phenomena. Low values of A_{mush} ($<10^5$) resulted in unrealistic predictions of the melt front development, higher values of A_{mush} ($>10^6$) corresponded to delayed melting of the PCM.
- In the early stages of melting, conduction is the dominant heat transfer mechanism, convection occurring when sufficient liquid PCM is formed.
- The predictions indicated that melting time decreased by 28.5 % when the wall flux was increased by 50 % from 500 to 750 W/m^2. The predicted time required for melting reduced by about 50% when the wall heat flux was increased from 500 to 1000 W/m^2.

7. Acknowledgements

The authors are grateful to the Engineering and Physical Sciences Research Council (EPSRC) for funding this work through Grant reference EP/N021304/1.

8. References

[1] S.P. Jesumathy, M. Udayakumar, S. Suresh, S. Jegadheeswaran, An experimental study on heat transfer characteristics of paraffin wax in horizontal double pipe heat latent heat storage unit, J Taiwan Inst Chem Eng. 45 (2014) 1298–1306. doi:10.1016/j.jtice.2014.03.007.

[2] A. Amini, J. Miller, H. Jouhara, An investigation into the use of the heat pipe technology in thermal energy storage heat exchangers, Energy. 136 (2017) 163–172. doi:10.1016/j.energy.2016.02.089.

[3] H. Niyas, S. Prasad, P. Muthukumar, Performance investigation of a lab scale latent heat storage prototype Numerical results, Energy Convers Manag. 135 (2017) 188–199. doi:10.1016/j.enconman.2016.12.075.

[4] H. Sattari, A. Mohebbi, M.M. Afsahi, A. Azimi Yancheshme, CFD simulation of melting process of phase change materials (PCMs) in a spherical capsule, Int J Refrig. 73 (2017) 209–218. doi:10.1016/j.ijrefrig.2016.09.007.

[5] S. Seddegh, S. Saeed, M. Tehrani, X. Wang, F. Cao, R.A. Taylor, Comparison of heat transfer between cylindrical and conical vertical shell-and-tube latent heat thermal energy storage systems, (2018). doi:10.1016/j.applthermaleng.2017.11.130.

[6] G.-S. Han, H.-S. Ding, Y. Huang, L.-G. Tong, Y.L. Ding, A comparative study on the performances of different shell-and-tube type latent heat thermal energy storage units including the effects of natural convection, (2017). doi:10.1016/j.icheatmasstransfer.2017.09.009.

[7] S. Jegadheeswaran, S.D. Pohekar, Performance enhancement in latent heat thermal storage system: A review, Renew Sustain Energy Rev. 13 (2009) 2225–2244. doi:10.1016/J.RSER.2009.06.024.

[8] H. Shokouhmand, B. Kamkari, Experimental investigation on melting heat transfer characteristics of lauric acid in a rectangular thermal storage unit, Exp Therm Fluid Sci. 50 (2013) 201–222. doi:10.1016/j.expthermflusci.2013.06.010.

[9] B. Kamkari, H. Shokouhmand, F. Bruno, Experimental investigation of the effect of inclination angle on convection-driven melting of phase change material in a rectangular enclosure, Int J Heat Mass Transf. 72 (2014) 186–200. doi:10.1016/j.ijheatmasstransfer.2014.01.014.

[10] P.H. Biwole, D. Groulx, F. Souayfane, T. Chiu, Influence of fin size and distribution on solid-liquid phase change in a rectangular enclosure, Int J Therm Sci. 124 (2018) 433–446. doi:10.1016/j.ijthermalsci.2017.10.038.

[11] A.D. Brent, V.R. Voller, K.J. Reid, Enthalpy-porosity technique for modeling convection-diffusion phase change: Application to the melting of a pure metal, Numer Heat Transf. 13 (1988) 297–318. doi:10.1080/10407788808913615.

[12] A.D. Brent, V.R. Voller, K.J. Reid, Enthalpy-Porosity Technique For Modeling Convection-Diffusion Phase Change: Application To

The Melting of A Pure Metal, Numer Heat Transf. 13 (1988) 297–318. doi:10.1080/10407788808913615.
[13] J. Vogel, J. Felbinger, M. Johnson, Natural convection in high temperature flat plate latent heat thermal energy storage systems, Appl Energy. 184 (2016) 184–196. doi:10.1016/j.apenergy.2016.10.001.